Elsevier Editorial System(tm) for Construction & Building Materials
Manuscript Draft

Manuscript Number: CONBUILDMAT-D-19-10308R2

Title: Thermo-mechanical and moisture absorption properties of fly ash-based lightweight geopolymer concrete reinforced by polypropylene fibers

Article Type: Research Paper

Keywords: lightweight geopolymer concrete; thermal insulation; fly ash; fiber reinforcement; thermo-mechanical properties; moisture absorption

Corresponding Author: Dr. Yijiang Wang,

Corresponding Author's Institution: State key laboratory for Geomechanics and Deep Underground Engineering

First Author: Yijiang Wang

Order of Authors: Yijiang Wang; Tongda Zheng; Xiaofeng Zheng; Yifei Liu; Jo Darkwa; Guoqing Zhou

Abstract: An experimental investigation on the thermo-mechanical and moisture absorption properties of lightweight geopolymer concrete prepared with fly ash, NaOH, sodium silicate and Polypropylene Fibers (PF) is presented in this study. The effects of dry density, NaOH, PF, aggregates and hydrophobic agent on the compressive strength, thermal properties and moisture absorption were studied. Results indicate that thermo-mechanical properties of Fly ash-based Lightweight Geopolymer Concrete (FLGC) strongly depend on the dry density, NaOH, PF and aggregates contents. The increase in dry density and fine aggregate contents resulted in higher compressive strength and thermal conductivity. NaOH within mass ratio of 0-10% is able to enhance thermo-mechanical properties. The optimal compressive strength was achieved when the length and content of the PF was 12 mm and 0.5% respectively. Meanwhile, PF in the range of 0-1% can also increase thermal conductivity and enhance moisture absorption. The increase in coarse aggregate ranging from 0 to 15% led to reduced dry density and thermal conductivity and enhanced moisture absorption, but did not affect compressive strength. Interestingly, the decrease in fine aggregate with the same content had the opposite impact to the moisture absorption in comparison to the coarse aggregate. However, the moisture absorption can be considerably weakened by surface waterproofing treatment which makes the enhanced thermal performance durable. Therefore, the FLGC reinforced by PF has excellent thermo-mechanical properties and can also be engineered to be an environmentally friendly and durable thermal insulation material with the assistance of waterproofing treatment.

Thermo-mechanical and moisture absorption properties of fly ash-based lightweight geopolymer concrete reinforced by polypropylene fibers

Yijiang Wang [a, b] *, Tongda Zheng [a], Xiaofeng Zheng [b], Yifei Liu [c], Jo Darkwa [b], Guoqing Zhou [a] *

[a] State key laboratory for Geomechanics and Deep Underground Engineering, School of Mechanics and Civil Engineering, China University of Mining and Technology, Xuzhou 221116, China

[b] Faculty of Engineering, University of Nottingham, University Park, Nottingham NG7 2RD, UK

[c] Shanghai Architectural Design and Research Institute, China State Construction Engineering Corporation, Shanghai 200062, China

Abstract: An experimental investigation on the thermo-mechanical and moisture absorption properties of lightweight geopolymer concrete prepared with fly ash, NaOH, sodium silicate and Polypropylene Fibers (PF) is presented in this study. The effects of dry density, NaOH, PF, aggregates and hydrophobic agent on the compressive strength, thermal properties and moisture absorption were studied. Results indicate that thermo-mechanical properties of Fly ash-based Lightweight Geopolymer Concrete (FLGC) strongly depend on the dry density, NaOH, PF and aggregates contents. The increase in dry density and fine aggregate contents resulted in higher compressive strength and thermal conductivity. NaOH within mass ratio of 0-10% is able to enhance thermo-mechanical properties. The optimal compressive strength was achieved when the length and content of the PF was 12 mm and 0.5% respectively. Meanwhile, PF in the range of 0-1% can also increase thermal conductivity and enhance moisture absorption. The increase in coarse aggregate ranging from 0 to 15% led to reduced dry density and thermal conductivity and enhanced moisture absorption, but did not affect compressive strength. Interestingly, the decrease in fine aggregate with the same content had the opposite impact to the moisture absorption in comparison to the coarse aggregate. However, the moisture absorption can be considerably weakened by surface

waterproofing treatment which makes the enhanced thermal performance durable. Therefore, the FLGC reinforced by PF has excellent thermo-mechanical properties and can also be engineered to be an environmentally friendly and durable thermal insulation material with the assistance of waterproofing treatment.

Keywords: lightweight geopolymer concrete; thermal insulation; fly ash; fiber reinforcement; thermo-mechanical properties; moisture absorption

1. Introduction

As the impact of climate change is causing great concern globally, there has been an increasing pressure on cutting carbon emissions across all sections. Currently almost 40% of the total world's energy consumption is contributed by the building sector, which is also responsible for 1/3 of total greenhouse gases emission [1]. Hence, the usage of energy saving and efficient materials has attracted increasing attention in the construction industry due to the need for a decarbonized building sector. The optimization in thermal properties of construction materials has been proved to be a crucial way to improve the durability and energy efficiency of buildings [2]. In addition, researchers have shown increased interest in construction materials with reduced environmental impact at both fabricating and operational stages of the material lifecycle [3]. For instance, one of the important implementations is the production of thermal insulation materials from solid wastes.

Coal fly ash is a type of fine solid particulate residue driven out of the boiler with the flue gases in coal-fired power plants. The disposal of fly ash is a major economic and environmental burden due to its abundance and release of toxic metals. The production of coal fly ash in China had been gradually increased from 5.32×10^8 t (2013) to 6.20×10^8 t (2015) and 6.86×10^8 t (2017). However, fly ash is a potential source of rare earth metals, which can be used for making geopolymer that resemble a cement-like product [4]. The geopolymer technology provides an alternative good solution to the utilization of fly ash with minor negative impact on the environment [5]. McLellan et al [6] presents an examination of the lifecycle cost and carbon impacts of ordinary Portland cement and geopolymers in Australian. Results show that the geopolymer concrete mixes based on typical feedstocks indicate potential for a 44-64% reduction in greenhouse gas emissions.

A considerable amount of research has been undertaken to make use of the industrial wastes such as fly ash to produce thermally and mechanically enhanced construction materials to reduce the negative environmental impact of the industries using various approaches associated with different ingredients and preparation processes. The compressive strength and thermal conductivity of lightweight geopolymer concrete were observed to be reduced by the reduction of the density [7]. Palm shell [8, 9], fly ash [3, 10-14] and wood fiber [15] have been used to produce the lightweight geopolymer concrete, which showed better thermo-mechanical properties comparing with the normal Portland cement foam concrete with the same density. The thermo-mechanical properties of the product are also affected by ingredients and manufacturing process. Huang et al [16] concluded that the optimal ratio for thermal properties of foam, glass and sodium hydrate was 35:35:5, and curing temperature was 55°C. The contents of fine aggregate can significantly reduce the compressive strength, which was not desirably affected by the increase in molarity [17].

Apart from the aforementioned methods, fine glass particles, expanded polystyrene and other solid waste such as bottom ash, crumb rubber, clay brick and pumice aggregates have also been utilized in attempts to enhance the mechanical and thermal performance of lightweight concrete products and the researching findings showed it is easy to reduce thermal conductivity but mechanical strength can be compromised sometimes, which is similar with the effect of aforementioned methods using fly ash. Specimen prepared by recycled fine glass particles was observed to show better strength and thermal performance than that with sand aggregate [18].

Colangelo et al [19] found that the compressive strength and bending strength decreased with the increased content of polystyrene, and the thermal conductivity was significantly reduced in comparison to that of the samples containing normal weight micro-silica sand. Mechanical and thermal properties of lightweight geopolymer mortar with locally available waste materials including bottom ash, crumb rubber, clay brick and pumice aggregates were investigated by Wongsa et al [20-22], which exhibited better thermal insulation and fire resistance than that of normal aggregates. The production process can also be challenging, for instance, Sanjayan et al [23] indicated that the foaming reaction is too fast to prevent complete alkali activation of geopolymers and therefore many unreacted fly ash particles remains in highly aerated specimens leading to poor mechanical strength. In order to overcome that issue, Abdullah et al [24, 25] proposed that the geopolymer lightweight concrete samples cured at 60 °C produced the maximum compressive strength. Interestingly, the water absorption and porosity were reduced by 6.78% and 1.22% after 28 days.

This paper presents an experimental investigation on the thermo-mechanical and moisture absorption characterization of Fly ash-based Lightweight Geopolymer Concrete (FLGC) reinforced by polypropylene fibers, which is a further advancement of the previous researches on the lightweight geopolymer concrete. In this study, the lightweight geopolymer concrete was prepared with fly ash, alkali solution (sodium hydroxide and sodium silicate), foaming agent, aggregates (ceramsite and standard sand) and reinforced by polypropylene fibers. Foam-stabilizing agent was also utilized to improve the foam stabilization and reduce bubble cracking. The impacts of dry density, NaOH, polypropylene fibers and aggregates on the compressive strength and thermal conductivity were reported. In addition, the effects of fiber length, aggregates and hydrophobic agent on the moisture absorption properties were also investigated.

2. Methodology

2.1. Experimental materials

2.1.1. Foaming agent

Owing to the excellent performance of the surface activity and the surface tension of liquid, foaming agent generated by animal protein was employed in this study. The performance of bubbles caused by foaming agent strongly depends on foam expansion, stability and hydrophobic property. According to the Chinese Standard JG/T266-2011 for foamed concrete, these three parameters should accord with the following requirements shown in Table 1. The actual parameters of foaming agent in this study were also presented in Table 1, from which the technical index of the foaming agent used in the experiments can be observed to completely meet the recommended technology parameters.

Table 1

Recommended and actual parameters of the foaming agent.

Parameter	Foam expansion	Stability (1 h)	Hydrophobic property (1 h)
Definition	Ratio of the volume of foam with volume of liquid agent	The descent length of the foam column	The volume of the liquid from cracked bubbles
Recommended	> 20	≤ 10 mm	≤ 80 mL
Actual	30	8.8 mm	70 mL

2.1.2. Fly ash

According to the Chinse Standard of GB/T1596-2017, fly ash of Class II from a coal mine company was activated by using alkaline activator solution in this experiment. X-Ray Diffraction (XRD) was employed to test the minerals of fly ash. It can be seen from Fig. 1 that the main mineral components of fly ash are mullite, sillimanite, quartz. As is generally known, the activity of fly ash strongly depends on the contents of the aluminum-silicon materials such as mullite, sillimanite and quartz. The X-ray fluorescence (XRF) was used to accurately determine the detailed chemical compositions of fly ash and its contents. As illustrated in Table 2, the main chemical compositions of fly ash are Al_2O_3 and SiO_2 with mass contents of 26.2% and 55.2% respectively. In addition, owing to the lower contents of calcium, the degree of polymerization of the fly ash is very high and therefore alkaline solution is necessary for the structural disintegration.

Table 2

Chemical compositions of fly ash.

Molecular formula	Al_2O_3	SiO_2	Fe_2O_3	K_2O	CaO	MgO	K_2O	Na_2O
Contents (%)	26.2	55.2	3.106	1.879	1.73	1.45	2.857	0.35

As shown in Fig. 1 (a) and (b), the microstructure of the original fly ash was examined by the Scanning Electron Microscope (SEM), from which it can be seen that fly ash consists of spherical particles in various sizes. These particles, with radius smaller than 10 μm, are usually hollow and may contain smaller particles in their interior spatial structure [26]. The surface of fly ash particles appears to be smooth, and some vitreous and quartz particles can also be observed [24].

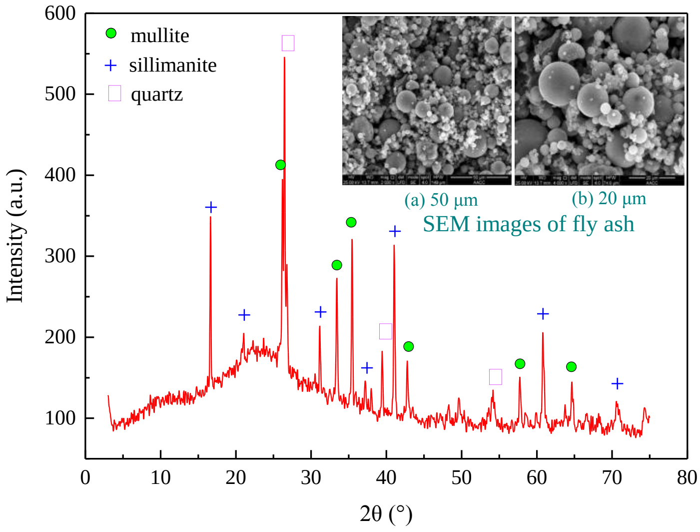

Fig. 1. XRD and SEM of fly ash.

2.1.3. Alkaline solution

The mesh structures of silicon and aluminum materials in the fly ash need to be disintegrated and activated by strong alkaline solution to produce the geopolymer concrete. The sodium hydroxide and sodium silicate solutions with mass concentration of 27.5% and modulus of 2.3 were prepared as the alkaline activator in this study.

Sodium silicate also called water glass which is a compound containing sodium oxide (Na_2O) and silicon dioxide (SiO_2) that forms a glassy solid with the very useful property of being readily soluble in water. The higher the ratio of SiO_2 to Na_2O and the higher the concentration of both ingredients, the more viscous the solution. The various grades of sodium silicate are characterized by their SiO_2:Na_2O molar ratio. Grades with molar ratio below 2.85:1 are generally termed alkaline. In this study, the molar ratio of sodium silicate solution is 2.3 so the sodium silicate solution can be used as alkaline solution.

2.1.4. Polypropylene fiber

Due to the high performance of abrasion resistance, corrosion resistance and fire resistance, PF has been usually chosen to reinforce the mechanical strength of lightweight concrete such as compressive and tensile strengths but without obviously increasing the corresponding thermal conductivity. The mechanical parameters of the PF are illustrated in Table 3, which shows that the tensile strength of the PF is much larger than the compressive strength of lightweight concrete. Consequently, the PF is an excellent material to reinforce the mechanical properties of lightweight concrete.

Table 3

Parameters of polypropylene fiber.

Density (g/cm^3)	Diameter (mm)	Tensile strength (MPa)	Modulus of elasticity (MPa)	Elongation at break (%)
0.91	0.017	461	4987	19

2.1.5. Aggregate and Additive agents

Standard sand and ceramsite were served as the fine and coarse aggregates, and the corresponding physical properties are listed in Table 4 and Table 5 respectively.

Table 4

Physical properties of standard sand.

Grain density (kg/m^3)	Dry density (kg/m^3)	Mean grain size (mm)	Void ratio	nonuniform coefficient
2643	1430-1740	0.39	0.52-0.85	1.542

Table 5

Physical properties of coarse aggregate.

Particle size (mm)	Bulk density (kg/m^3)	Apparent density (kg/m^3)	Water absorption-1h (%)	Cylinder compressive strength (MPa)
5-10	520-540	780-800	8.7	2.8

In addition, modified polyethoxylated silicone and silicone-based hydrophobic agents were used as the foam-stabilizing agent and hydrophobic agent in this study. Silicone-based hydrophobic agents can attach very readily to surfaces and have a very high spreadability. Foam-stabilizing and hydrophobic agent were utilized to improve the foam stabilization, reduce bubble cracking and enhance the waterproof capacity.

2.2. Experimental scheme

2.2.1. Experimental programme

According to the pre-experimental results, the mass ratio of total water to fly ash was set as 0.4. It should be noted that the above-mentioned total water includes the water in alkaline solutions and additional portion added into the concrete. In addition, the mass ratio of fly ash to sodium silicate was set as 4. The mass ratio of NaOH to fly ash in the range of 5%-20% was made to investigate the impact of the amount of NaOH on the thermo-mechanical properties of lightweight geopolymer concrete. The amount of aggregate and PF is based on the mass of geopolymer concrete. The detailed experimental programme is presented in Table 6.

Table 6

Experimental programme.

No.	Fly ash (g)	Na_2SiO_3 (g)	NaOH (%)	Aggregate (%)	Foam (L)	PF (%)	Fiber length (mm)
A	6000	1500	10	—	0~12	0.5	3
B	6000	1500	5/10/15/20	—	6	0.5	3
C	6000	1500	10	—	6	0.5	0/3/6/9/12/19
D	6000	1500	10	—	6	0/0.5/1.0/1.5	3
E	6000	1500	10	—	6	0/0.5/1.0/1.5	12
F	6000	1500	10	0/5/10/15 (fine)	6	0.5	3
G	6000	1500	10	0/5/10/15 (coarse)	6	0.5	3
H	6000	1500	10	—	6	0.5	3/6/12/19
I	6000	1500	10	—	6	0.5/1.0/1.5/2.0	3

2.2.2. Experimental procedures

The experimental procedures for producing the fiber-reinforced FLGC include five steps: (1) raw material preparation, (2) foaming, (3) stirring, (4) casting mould/curing and (5) demoulding. More details about the procedures are listed in Table 7.

Table 7

Details of experimental procedures.

Steps	Detailed procedures
(a) Raw material preparation	The mass of fly ash and sodium silicate were kept constant at 6000 g and 1500 g in this study respectively. The sodium hydroxide was mixed with water and then cooled to room temperature. Aggregate and PF are then measured by an electronic scale.
(b) Foaming	The foam agent was fed into the foaming machine with optimal foaming pressure of 0.5MPa and foam expansion ratio of 1:40 to produce the foam which was measured by a measuring glass.
(c) Stirring	The pre-measured raw materials including fly ash, sodium hydroxide solution, sodium silicate solution, PF and foam were orderly added into the blender to stir for about 8-9 minutes.
(d) Casting mould and curing	The slurry was poured into 100 mm ×100 mm ×100 mm plastic molds. The wet density of samples was tested. The samples with plastic molds were moved to a curing chamber with relative humidity of no less than 90% and temperature of 20 ± 1℃ for 24 h.
(e) Demoulding	After the curing, these samples were demoulded and then placed at room temperature to wait for the experimental tests.

2.2.3. Testing method and data processing

The wet density, apparent density and dry density of samples were calculated using the ratio of the samples' mass to the mould's volume. The 28 days compressive strength of samples was evaluated according to GB/T11969-2008. The two ends of all the samples were grinded to be in parallel and normal to the height to avoid the stiffening effect that could be caused by uneven end surfaces of the sample during the initial stage. The results reported herein are the average of the three measurements of the strength. The compressive strength was tested by an electro-hydraulic servo testing machine with 2000 kN capacity.

The microstructural characterization was examined with the aid of SEM and 3D Digital Microstructure (3D-DM) respectively. XRD and XRF were used to characterize the detailed minerals and chemical compositions of samples. The diffraction patterns were analyzed and identified with the assistance of the corresponding software program. Thermal conductivities of samples were measured by a thermal constants analyser based on the theory of the transient plane source. In addition, the thermal conductivity, thermal diffusivity as well as specific heat per unit volume can be obtained from one single transient recording and the agreement was considered exceptionally good compared with any other experimental technique [27].

Water content tests were conducted through weighting the mass of samples with different moisture according to JGJT70-2009. The mass ratio between hydrophobic agent and water was 1:10. All the demoulded samples were put into an oven with temperature of 65±2 ^{o}C for 24 h, and then dried in the oven with temperature of 105±5 ^{o}C for another 24 h. To avoid damage to the surface waterproofing layer, the dried samples were conducted by surface waterproofing and then naturally dried for 24 h. The dried samples with and without surface waterproofing were put into an environment chamber with constant temperature and relative humidity. When the moisture content test was conducted, the samples should be removed from the chamber and weighted by an electronic balance with accuracy of ±0.01g. In order to reduce the influence of indoor environment on the moisture contents, each specimen was tested only once.

To ensure the accuracy of the experimental results, the testing accuracy and uncertainties of the experimental setup are analyzed and presented in Table 8. The uncertainties were computed through the testing accuracy and the Bessel equation of standard deviation. The equations of uncertainties for directed variables are presented by [28]:

$$u_{\mathrm{v}} = \sqrt{\Delta_{\mathrm{v}}^2 + \sigma_{\mathrm{v}}^2} \quad (1)$$

where u_{v} is uncertainty of directed variables, Δ_{v} is the test accuracy of the variables, σ_{v} is the Bessel equation of standard deviation and the equation is shown:

$$\sigma_{\mathrm{v}} = \sqrt{\frac{\sum_{i}^{N}(x_i - \bar{x})^2}{N-1}} \quad (2)$$

where x_i and $\bar{x}$ are individual testing values and the mean value of individual testing values, N is the number of testing items.

Table 8

Accuracies and uncertainties of testing variables.

Variables	Thermal conductivity	Compressive strength	Mass
Testing accuracy	±2%	±1%	±0.01 g
Uncertainty	±5%	±7%	-

The measurement uncertainties of thermal conductivity and compressive strength are ±5% and ±7% based on calculated data respectively, which can ensure the accuracy of the experimental set. In addition, the standard deviation is also calculated to quantify the divergence of experimental results.

3. Results and discussions

3.1. Thermal conductivity and compressive strength

3.1.1. Dry density

Table 9 shows the variation of dry density with foam contents (group A in Table 6). It is clearly that the dry density of the lightweight geopolymer concrete is nonlinearly decreased by the increased volume of foam added into the FLGC. The amount of added foam should be carefully selected in order to acquire the lightweight geopolymer concrete with excellent compressive strength and thermal conductivity.

Table 9

Dry density versus foam volumes.

Foam volumes (L)	0	2	4	6	8	10	12
Dry density (kg/m^3)	1722	1503	1299	858	662	554	498

Thermal conductivity and compressive strength, which are the two most important physical properties of thermal insulation materials, strongly depend on the dry density of the samples, which results from the volume of foam added into the FLGC. The thermal conductivity and compressive strength of samples with different dry densities are illustrated in Fig. 2, in which it can be seen that the compressive strength and thermal conductivity nonlinearly reduced as the dry density decreased. It was also observed that the compressive strength and thermal conductivity significantly decreased when the dry density was reduced in the range of 858 kg/m^3-1722 kg/m^3. For example, the compressive strength and thermal conductivity of the sample with dry density of 1722 kg/m^3 was 7.20 MPa and 1.14 W/(m·K), which was 4.1 and 5.4 times larger than those of the one with dry density of 858 kg/m^3 respectively. The reason is that the connection between FLGC gels was broken by the air bubbles as the foam was added into the FLGC. The compressive strength of FLGC samples was shown to be apparently decreased by the decreased dry density. The air bubbles in the samples were full of air with lower thermal conductivity than that of FLGC. Hence, the effective thermal conductivity of samples also considerably decreased when the dry density decreased. The decreasing rate of thermal conductivity and compressive strength of FLGC samples were not so significant when the dry density was lower than 858 kg/m^3. It was observed that the compressive strength and thermal conductivity respectively decreased from 1.75 MPa and 0.21 W/(m·K) to 0.95 MPa and 0.095 W/(m·K) when the dry density was decreased from 858 kg/m^3 to 498 kg/m^3. Both approached the lower limits when the dry density decreased to around 498 kg/m^3, at which point it is not feasible to further reduce the thermal conductivity by increasing the volume of the foam which leads to decreased dry density and compressive strength.

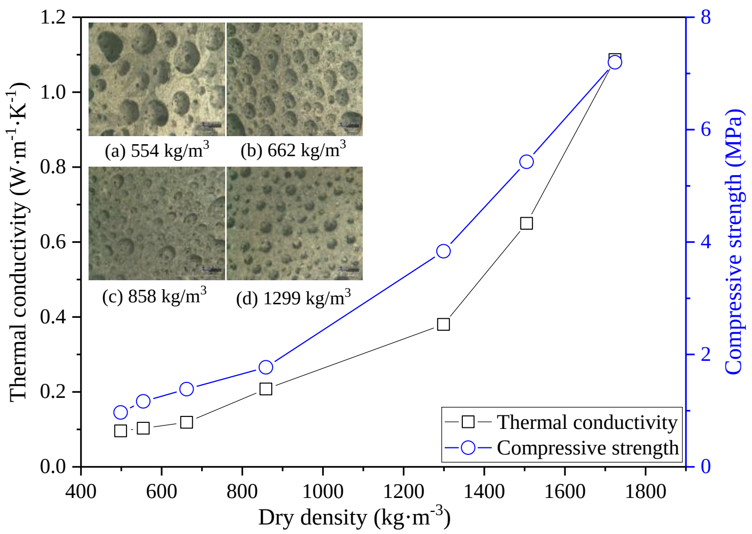

Fig. 2. Variations of thermal conductivity and compressive strength of FLGC with dry density.

3D-DM was conducted to investigate the pore structures of the FLGC samples. Four cubic samples with density of 554 kg/m^3, 662 kg/m^3, 858 kg/m^3 and 1299 kg/m^3 were selected for the investigations which are shown in Fig. 2 (a, b, c & d). It can be seen from the microstructural images of four samples that most air voids are approximately spherical in shape. These air voids are not of uniform size and the diameter of the largest air voids was observed to be increased by the decreased dry density. The air voids in four samples with different dry densities consist of two types of air bubbles which are called closed and merged air voids respectively. The closed air voids are those that are fully covered with the binder paste, and the merged air bubbles are those resulted from the combination of more than two adjacent air voids [29]. As illustrated in Table 9, the dry density of samples was decreased when the volume of the foam added into the FLGC increased, which suggests that the porosity of samples has a strongly positive correlation with the dry density. As the dry density of samples decreases, the distances between two or more than two air voids decreased, while the number of those adjacent air bubbles increased. Consequently, the probability of merging adjacent air bubbles to form air voids of larger diameter was considerably increased. As shown in Fig. 2(a) and (d), the diameter of the largest air bubble in the sample with dry density of 554 kg/m^3 can be up to 1300 μm which is about six times larger than that formed with a dry density of 1299 kg/m^3.

Fig. 3 demonstrates the distribution of the diameter of air bubbles in the samples with different dry densities shown in Fig. 2 (a, b, c & d) which was counted using the software of 3D-DM. As can be seen from Fig. 3, the air voids with diameter in the range of 300-500 μm account for the largest proportion, and decrease with decreasing dry density. The air bubbles with diameter larger than 1000 μm were only observed in samples with dry density lower than 858 kg/m^3. The reason was that the adjacent air bubbles with smaller diameters merged to generate air voids with larger diameter. The air bubbles with larger diameter could be therefore observed in the samples with lower dry density. Although the percentage of the air bubbles with larger diameter was obviously less than that with smaller diameter, the area or volume occupied by air voids with larger diameter were hundreds of thousands of times larger than those of smaller air bubbles.

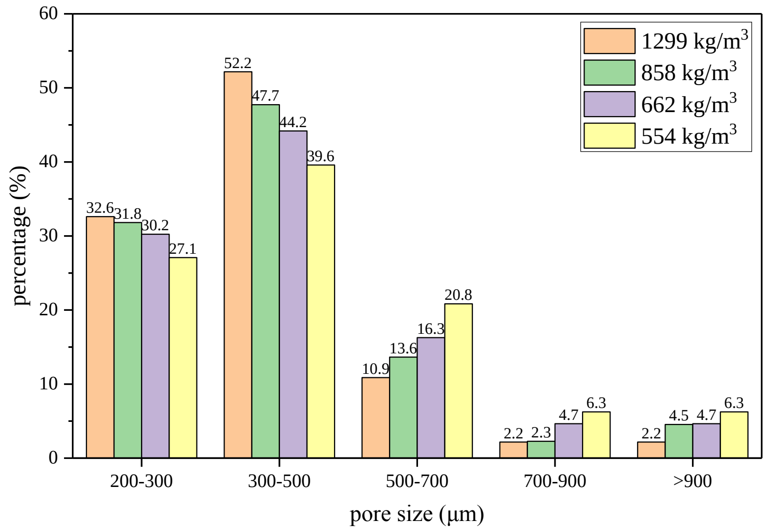

Fig. 3. Pore size distribution with different dry densities.

According to the variations of compressive strength and thermal conductivity of FLGC shown in Fig. 2, the samples with dry density ranging in 500-600 kg/m^3 were prepared to investigate the variation of thermo-mechanical and moisture absorbing properties hereafter.

3.1.2. NaOH contents

As the main alkaline activated materials, the contents of NaOH is commonly believed to be one of the most significant factors affecting the thermo-mechanical properties of lightweight geopolymer concrete [30, 31]. Fig. 4 demonstrates the influence of the mass ratio of NaOH to fly ash on the compressive strength and thermal conductivity of the lightweight geopolymer concrete (group B in Table 6). An increase in the thermal conductivity of FLGC samples was observed when NaOH contents increased. It appears that the effects of NaOH contents on compressive strength in this study differed from previous observation, which suggested there is a monotonic increasing or decreasing relationship between compressive strength and NaOH concentration [32]. However, the results herein revealed the compressive strength was increased firstly and then decreased as the contents of NaOH increased from 5% to 20%. In details, the maximum compressive strength 1.38 MPa was achieved when the NaOH content was 10%. When the contents of NaOH were larger than

10%, the compressive strength of the samples was observed to be decreased by increased NaOH contents which agrees with the experimental results in previous literatures [33].

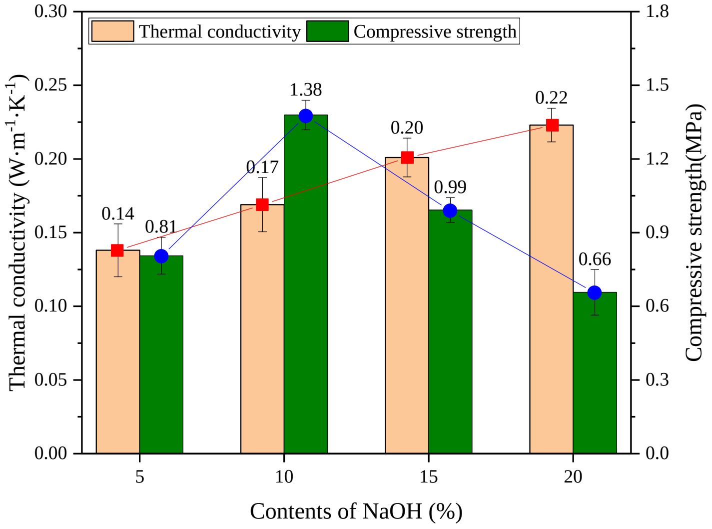

Fig. 4. Thermal conductivity and compressive strength versus NaOH contents.

Lower NaOH contents resulted in the insufficient geo-polymerization between the fly ash and alkali solutions. As shown in Fig. 5 (a), the fly ash was clearly seen not to be completely dissolved by alkali solutions, and a large number of micro-cracks which could limit the strength of geopolymer were also found in the matrix. Owing to the insufficient geo-polymerization, the compressive strength of final products with NaOH contents of 5% was therefore not high. Dissolution of fly ash was accelerated when the NaOH was sufficient, which in this case study is 10%. Fly ash particles were not easily noticed as most particles were fully dissolved and covered with geopolymer gel, as shown in Fig. 5 (b). It formed a continuous mass of gel which resulted in a relatively dense geopolymer paste with higher compressive strength [30]. As shown in Fig. 5 (c, d), the excess hydroxide ion concentration from higher NaOH contents led to aluminosilicate gel precipitation at the very early stages [32, 33]. The leaching of silicon and aluminum in fly ash was hindered. The geo-polymerization was consequently obstructed which resulted in negative impact on the compressive strength.

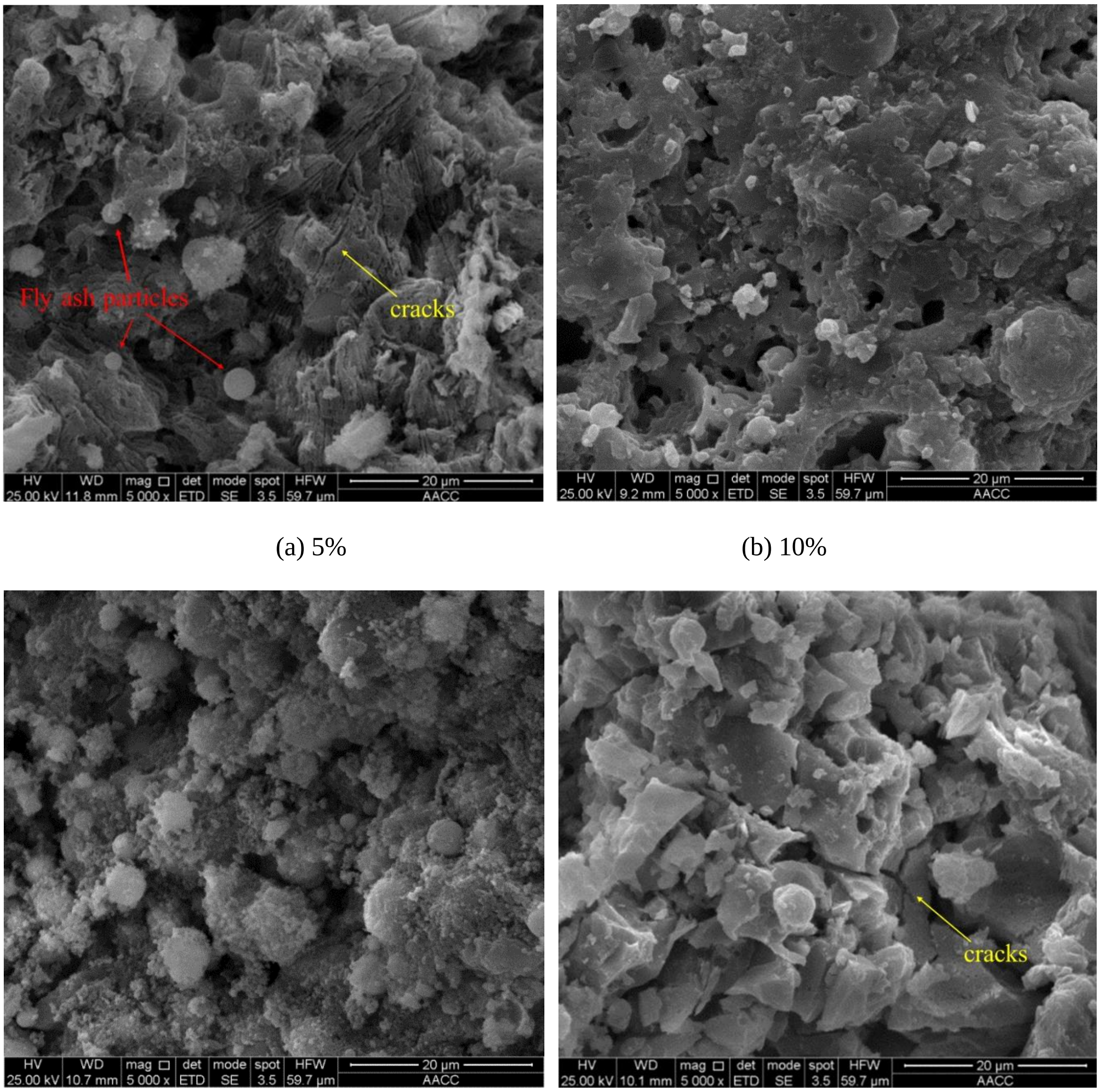

(a) 5% (b) 10%

(c) 15% (d) 20%

Fig. 5. SEM of FLGC versus NaOH contents.

The comparison of XRD results between the FLGC samples with different NaOH contents and fly ash is presented in Fig. 6. It is clear that the patterns of FLGC are similar to that of fly ash, which indicates that the degree of amorphous and crystallization of fly ash was not noticeably changed by geo-polymerization. The amount of crystal of quartz and mullite from geopolymer which mainly consisted of amorphous aluminosilicate products was similar or very slightly increased to those from fly ash [30]. There are two main differences between XRD patterns of lightweight geopolymer concrete and fly ash. The first one is the shift of amorphous sillimanite peak from around 25-28° for FLGC and fly ash, which indicates that the silicate glass phase in FLGC was highly disordered. Another point to be aware of is graphics of FLGC at 5-8° curved slightly upwards compared to that of fly ash. This could be the formation of meso-materials of poorly crystalline nature [34].

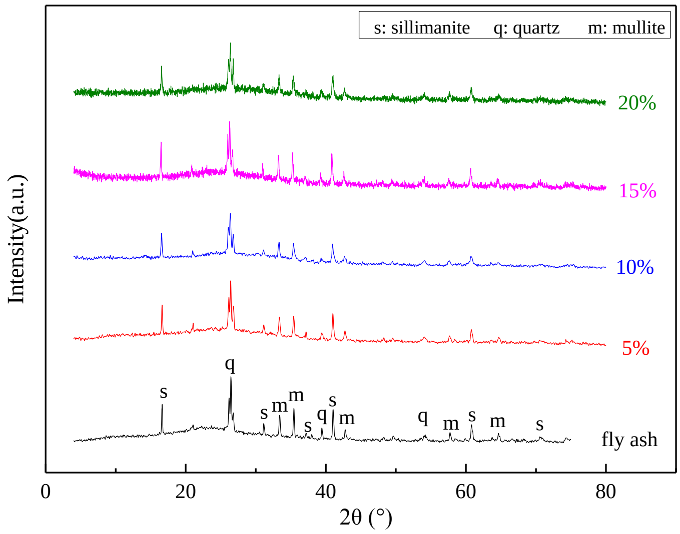

Fig. 6. The XRD of FLGC versus NaOH contents.

3.1.3. Polypropylene fiber

Fiber reinforcement in lightweight concrete was widely believed as one of the most effective way to improve its properties, such as flexural capacity, toughness, post-failure ductility and crack control [35]. Fibers can be categorized as metallic, glass, polymeric, carbon, mineral and asbestos. Among the various types of fibers, polypropylene fiber is the most commonly used for thermal insulation purposes. Other reasons for the greater usage of PF also include economical advantage and excellent resistance to environmental aggressiveness.

Fig. 7 presents the impact of PF length on the improvement of compressive strength of lightweight geopolymer concrete on 28 days (groups C/D/E in Table 6). It is seen from the figure that the compressive strength of fiber reinforced FLGC with fiber lengths of 3 mm, 6 mm, 9 mm, 12 mm and 19 mm was increased by 57%, 46%, 57%, 71% and 6% respectively comparing to the samples without PF. Hence, it suggests that the compressive strength strongly depends on the fiber length. The high performance in compressive strength of fiber reinforced lightweight geopolymer concrete might be achieved by the PF that mechanically interacted with the FLGC. When the uniaxial load applied on the sample exceeded its peak stress, cracks were observed on the surface and interior of the cubic specimen. As typical observation from fiber reinforced FLGC specimens shown in Fig. 8, crack tips in FLGC samples would be concatenated by fibers, resulting in decreasing the number of cracks and blocking the propagation of existing cracks [36]. The compressive strength of lightweight geopolymer concrete was therefore increased by PF.

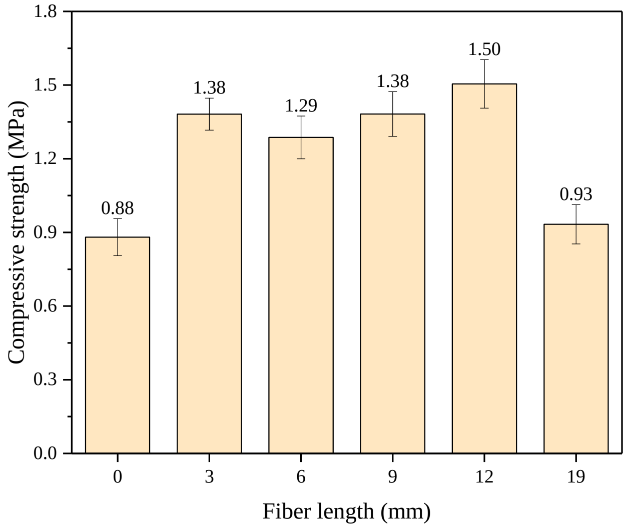

Fig. 7. Effects of fiber length on compressive strength.

Residual compressive strength of cracked fiber reinforced FLGC provides a clearer comparison of the post cracking behaviors. As seen from Fig. 8, the specimen without fibers had the lowest residual compressive strength owing to the deficiency of fiber-concrete bond. The post-failure compressive strength of specimen without PF was decreased to 25% of the peak strength with the axial displacement of 5 mm. Meanwhile, the post-failure compressive strength of samples with PF of 12 mm for the second and third load strength reduced to 90%, 91% with axial displacement of 1.4 mm and 1.9 mm respectively, which is about 1.55 times larger than the peak strength of specimen without fibers. This might be attributed to that the bridging effect of fibers at the crack face is capable of preventing cracks from propagating [37].

In addition, the failure forms of fiber reinforced specimens and samples without fibers significantly varied, as shown in Fig. 8. Vertical cracks appeared first around the mid-height of the cubic FLGC specimen without fibers, and diagonally propagated to four corners with a further increasing uniaxial loads. Obvious spalling fragments of FLGC without fibers were observed under the peak compressive loads. This kind of failure configuration of FLGC without fibers was truncated pyramids or brittle failure [38]. It is seen that there was no obvious spalling concrete in fiber reinforced FLGC compared with those samples without fibers. This may be related to the bridge action of fibers, indicating that the lateral deformation could be constrained by the addition of fibers. The data in Fig. 7 and Fig. 8 verified that the addition of fibers not only improved the compressive strength of FLGC, but also changes its failure configuration [39].

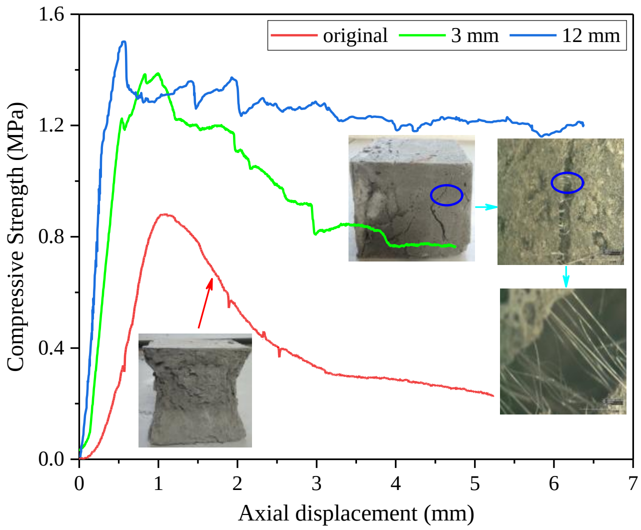

Fig. 8. Stress-displacement curves for different fiber lengths.

The variations of compressive strength and thermal conductivity of fiber reinforced FLGC with various PF contents are presented in Fig. 9. The compressive strength of fiber reinforced FLGC first increased and then decreased when the PF contents increased from zero to 2%, with a critical point for the PF contents of 0.5%, where the internal structure of FLGC was considerably improved. Similar variation for thermal conductivity with PF contents is also observed in Fig. 9 (b). The main reason for the decrease in the compressive strength when the PF contents is greater than 0.5% is that the dispersion of fiber, especially in high volume fractions is very difficult and consequently causes poor workability and incomplete compaction [39].

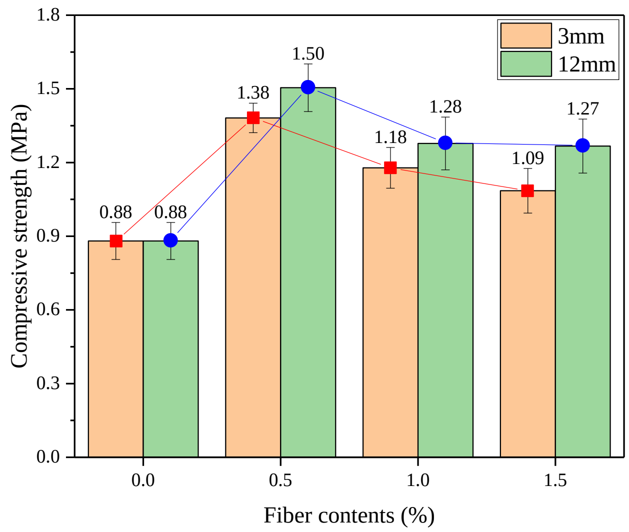

(a) Compressive strength

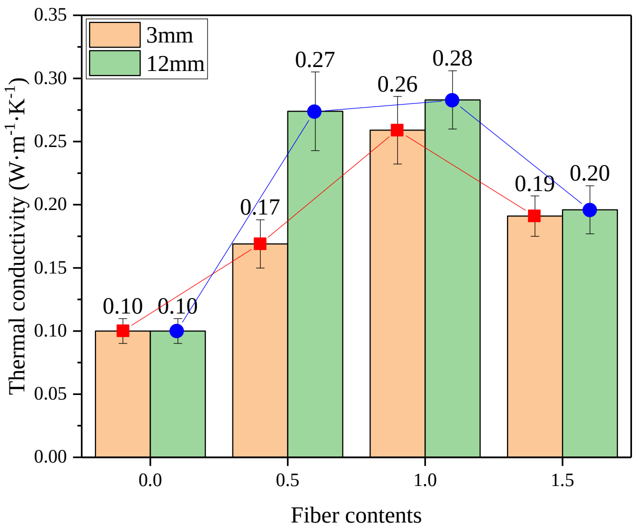

(b) Thermal conductivity

Fig. 9. Compressive strength and thermal conductivity versus fiber contents.

Besides, the compressive strength and thermal conductivity of fiber reinforced FLGC with fiber length of 12 mm were observed to be slightly higher than that of 3 mm. The contact area between fibers and geopolymer concrete increased with increasing fiber length, which resulted in larger frictional force and preferable performance of bridge effects of longer fibers. More air voids could be linked through longer fibers compared with shorter fibers. The thermal conductivity of samples with longer fibers was therefore increased.

3.1.4. Aggregates

Ceramsite fabricated by domestic sludge and standard sand in the city of Xiamen, was used as the coarse and fine aggregates respectively. The change of dry density and thermal conductivity of

FLGC with ceramsite and standard sand is illustrated in Fig. 10 (groups F/G in Table 6). It is obvious from Fig. 10 (a) that both the thermal conductivity and dry density of the samples with coarse aggregate were decreased steadily by the increased amount of additive. Increase in the contents of coarse aggregate from 0% to 15% resulted in the reduction of the thermal conductivity and dry density from 0.17 W/(m·K) to 0.086 W/(m·K) and 650 kg/m^3 to 480 kg/m^3 respectively. However, the opposite effect was given by fine aggregate. As shown in Fig. 10 (b), both the thermal conductivity and dry density were increased by the increase of contents of fine aggregate. For instance, increase in the contents of fine aggregate from 0% to 15% resulted in the increases of the thermal conductivity and dry density from 0.17 W/(m·K) to 0.21 W/(m·K) and 550 kg/m^3 to 660 kg/m^3 respectively.

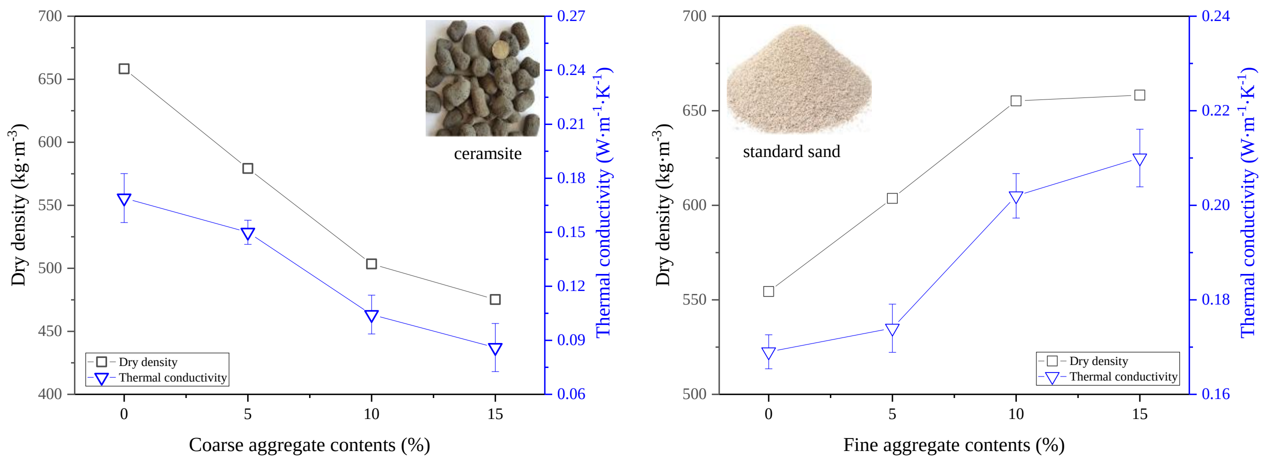

(a) ceramiste (b) standard sand

Fig. 10. Thermal conductivity and dry density versus aggregate contents.

Fig. 11 demonstrates the variation of compressive strength with the contents of coarse and fine aggregates. It is clear that the compressive strength of samples strongly depended on the amount of standard sand (fine aggregate). Increase in the contents of standard sand from 0% to 15% resulted in the increases of the compressive strength from 1.38 MPa to 2.6 MPa. However, the increase in the contents of ceramsite (coarse aggregate) from 0% to 15% did not significantly change the compressive strength.

The bulk density of ceramiste and standard sand was about 400 kg/m^3 and 1400 kg/m^3 respectively. Considering the dry density of the FLGC lies between the bulk densities of ceramsite and standard sand, adding the coarse or fine aggregates into the geopolymer concrete would therefore produce samples with quite different dry densities. Increase in the contents of coarse aggregate resulted in decrease of dry density, whilst increase of fine aggregate resulted in increase of dry density. As plotted in Fig. 2, it can be seen that dry density of the samples has a direct impact on the compressive strength, while the effects of coarse and fine aggregates on the compressive strength are essentially different. Similar explanation could also be applied to illustrate the variation of thermal conductivity with the contents of coarse and fine aggregates.

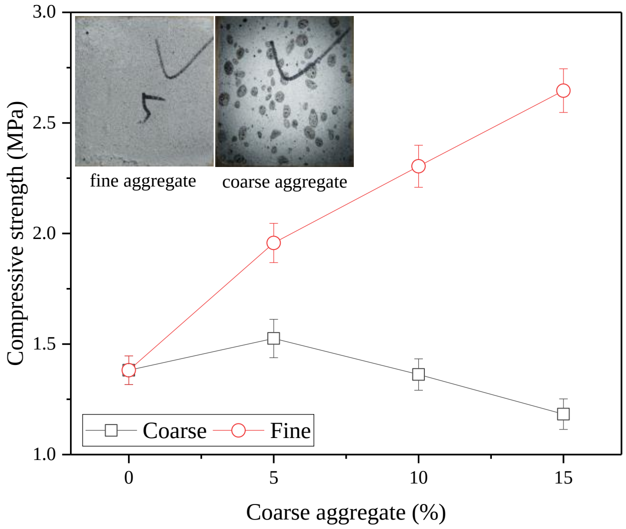

Fig. 11. Compressive strength versus aggregate contents.

3.2. Moisture absorption

One of the most important motivations for investigating the variation of moisture absorption is that the thermal conductivity of FLGC samples strongly depends on the moisture contents. Compared to the normal weight concrete, the lightweight concrete had higher moisture absorption owing to the lower dry density. According to our previous testing results, the thermal conductivity of FLGC specimen with mass water contents of 0%, 6% and 8% was gradually increased from 0.17 W/(m·K) to 0.28 W/(m·K) and 0.39 W/(m·K) respectively. Therefore, it is necessary to study the factors that affect the moisture contents.

3.2.1. Polypropylene fiber

Fig. 12 demonstrates the effects of fiber length and fiber contents on the moisture absorption of FLGC samples (groups H/I in Table 6). The FLGC samples with added fibers in different length were put in the chamber with dry bulb temperature of 35±0.3 ℃ and relative humidity of 80±1.5%, whilst the specimens mixed with 3 mm fibers at various levels of contents were placed in the chamber with dry bulb temperature of 35±0.3 ℃ and relative humidity of 90±1.5%.

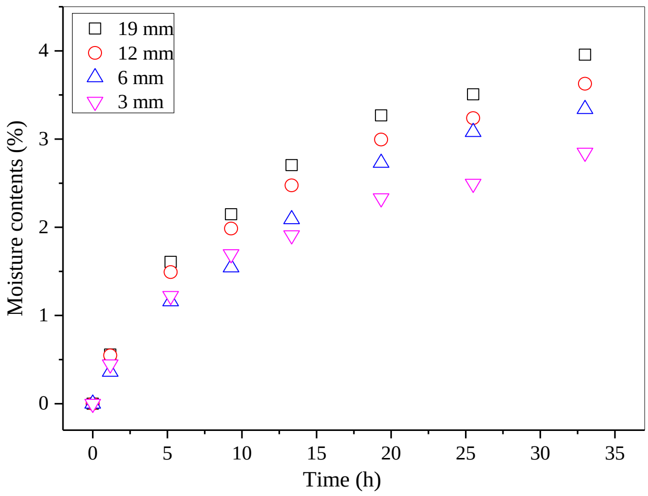

(a) fiber length

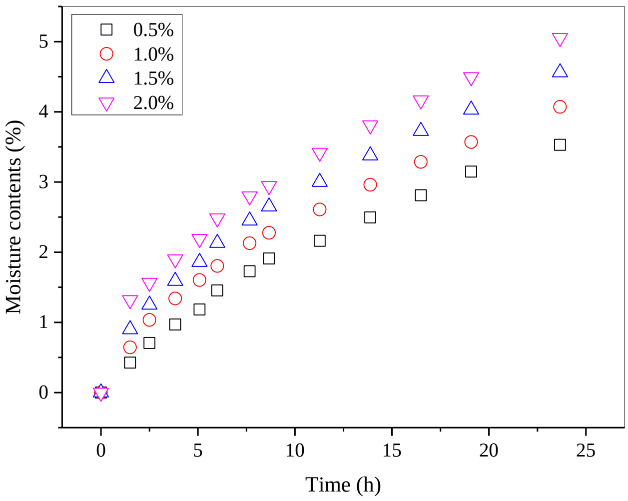

(b) fiber contents

Fig. 12. Moisture contents versus fiber length and fiber contents.

As shown in Fig. 12, the moisture contents of FLGC sample in the chamber with relative humidity of 90% is 3.14% at 19.1 h, compared with moisture contents of 2.33% at 19.3h with relative humidity of 80%. Hence, the moisture contents of FLGC samples was closely linked to the surrounding thermodynamic parameters including relative humidity. As shown in Fig. 12 (a), the moisture contents increased when the fiber length increased. In addition, the increase in the fiber contents resulted in higher moisture absorption capacity, as presented in Fig. 12 (b). It is widely accepted that the excellent performance of water absorption was achieved by the capillary effect of fibers in the FLGC. The fibers mixed into the FLGC samples were equivalent to the water-conducting channels. The moisture in the surrounding environment could be continuously diffused into the FLGC samples along the fibers. The length and number of the water conducting channels was believed to increase with the increased fiber length and fiber contents respectively. Consequently, the moisture absorption capability of samples could be improved by mixing longer fibers and larger amount of fibers into the FLGC.

3.2.2. Aggregates

Fig. 13 shows the impact of fine and coarse aggregates on the moisture absorption capacity of FLGC samples (groups F/G in Table 6). As shown in Fig. 13 (a), an increase in the contents of fine aggregate reduced the moisture absorption of FLGC specimens, which agrees with the finding shown in Fig. 10 (b), i.e. the dry density of FLGC samples was gradually increased when contents of fine aggregate increased. The larger dry density was attributed to lower volumes of pores and larger fraction of standard sand. The FLGC specimens with high dry density contained lower amount of air voids, and this defective porous structure consequently led to poorer moisture absorbing capacity. However, Fig. 13 (b) shows that increasing the amount of ceramsite resulted in higher moisture absorption. As shown in Fig. 10 (a), the dry density was decreased when the amount of coarse aggregate increased. The FLGC samples with lower dry density contained higher volume of coarse aggregates and air voids, which in consequence absorbed more moisture owing to their highly porous structures [2]. In addition, another reason was due to the physical properties of the ceramsite aggregates which have higher moisture absorption capacity due to increased specific surface area. Similar conclusions were drawn by Aslam et al [40] and Ahmmad et al [41] that water absorption of the concrete increased gradually by increasing the added amount of ceramite in lightweight concrete.

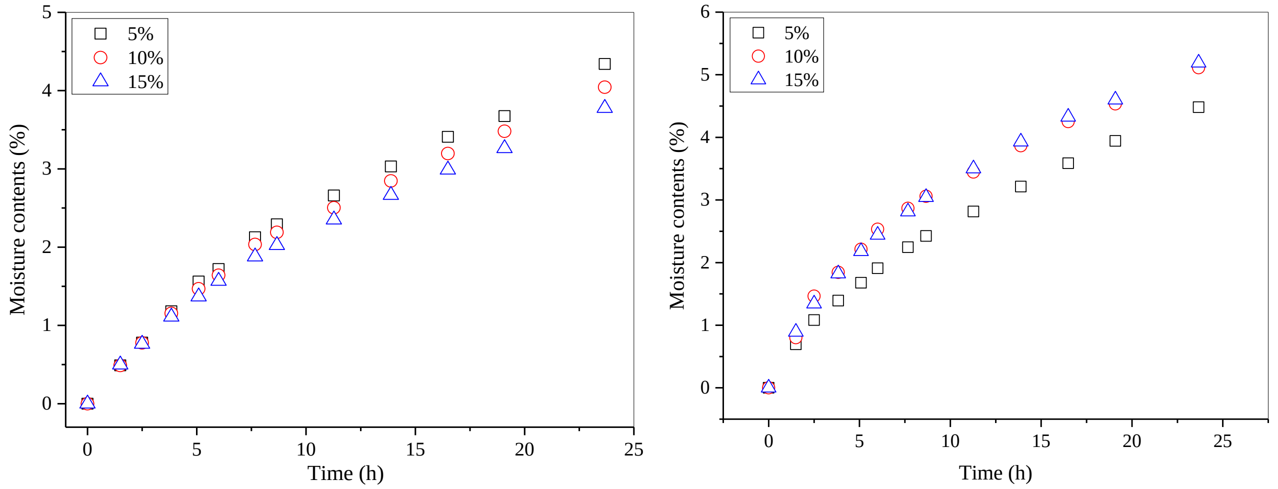

(a) fine (b) coarse

Fig. 13. Moisture contents versus aggregate contents.

3.2.3. Hydrophobic agent

Hydrophobic agent, which is surface protection materials and capable of increasing the angle of contact between the water droplet and the concrete surface [42], can be used to reduce liquid water penetration into the concrete and the thermal property of concrete is also not deteriorated. The hydrophobic agent with diluted concentration by 10 times was homogeneously sprayed onto the surface of the FLGC samples, and all specimens were naturally dried at room temperature. The waterproofing specimens were then put into the chamber with dry bulb temperature of 35±0.3 ℃ and relative humidity of 90±1.5% to investigate the effect of waterproofing treatment on moisture absorption of FLGC samples.

Fig. 14 presents the variation of moisture contents of waterproofing specimens with different fiber contents and the comparison of moisture contents of waterproofing sample with that of original specimen with the same fiber length of 3 mm (group D in Table 6). It is observed that the moisture absorption of waterproofing samples was considerably reduced compared with original samples shown in Fig. 12 (b). In addition, the effect of fiber contents on moisture absorption capacity of waterproofing samples also drastically decreased. For instance, the moisture content of waterproofing samples with fiber content of 0.5% was 0.93% at 23.7 h, compared with the moisture content of 3.52% for the untreated specimen with the same fiber contents at 23.7 h. Similar conclusions could also be drawn through the comparison of the moisture contents of waterproofing samples with fibers contents of 1.0 % and 1.5 % with those of original specimen with same fiber contents shown in Fig. 12 (b). The waterproofing treatment is therefore the most effective method to reduce the moisture absorption of FLGC samples.

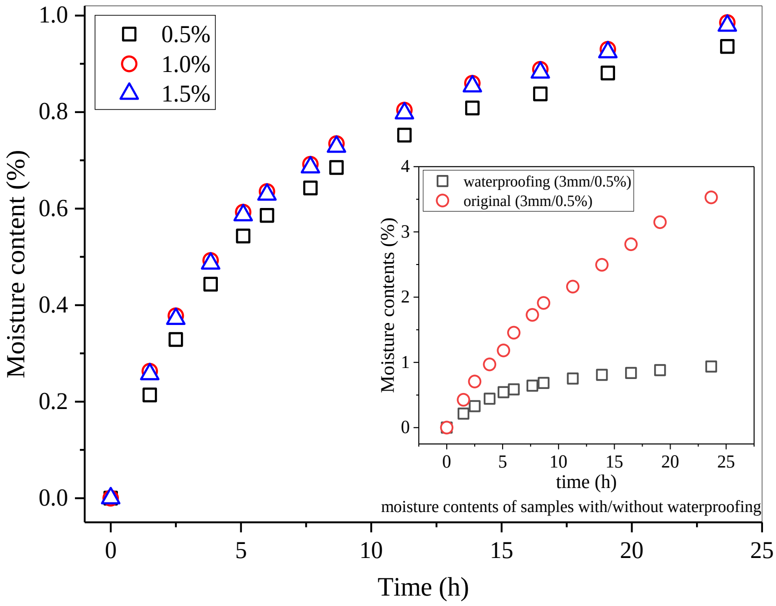

Fig. 14. Moisture contents of waterproofing samples versus fiber contents.

4. Conclusions

An experimental investigation on the thermo-mechanical and moisture absorption properties of lightweight geopolymer concrete prepared with fly ash, NaOH, sodium silicate solutions and polypropylene fibers was presented in this study. The main findings are as follows:

(1) The dry density of the lightweight geopolymer concrete nonlinearly decreased when the foam volume increased. The compressive strength and thermal conductivity generally nonlinearly reduced as the dry density decreased, which is probably intuitive. But it was found out that it is not

feasible to further reduce the thermal conductivity by increasing the volume of the foam as it would lead to poor binding because of excessively lower compressive strength when the dry density decreased to about 498 kg/m^3.

(2) The compressive strength increased firstly and then decreased when the contents of NaOH increased from 5% to 20%, the turning point was found to be at 10%. The excessive hydroxide ion concentration from higher NaOH contents led to aluminosilicate gel precipitation, which consequently weakened the compressive strength. It was observed that the thermal conductivity was consistently increased by the increased contents of NaOH. Therefore, NaOH can be used to enhance the compressive strength rather than thermal insulation performance.

(3) The compressive strength of fiber reinforced FLGC with fiber lengths of 3 mm, 6 mm, 9 mm, 12 mm and 19 mm was respectively increased by 57%, 46%, 57%, 71% and 6%. This suggests the addition of fiber is able to enhance the compressive strength of FLGC owing to the bridging effect of fibers at the crack face. In addition, the enhancement is less obvious when the fiber length exceeds 12 mm as the longer polypropylene fibers were difficult to uniformly disperse in the FLGC which resulted in the anisotropic sample. This similar finding was also applicable to the thermal conductivity, as both parameters first increased and then decreased when the fiber contents increased from zero to 2%.

(4) Increase in the contents of coarse aggregate from zero to 15% resulted in the reduction of the thermal conductivity and dry density. The opposite trend was observed with the fine aggregate, i.e. the thermal conductivity increased when the contents of fine aggregate increased because the dry density of samples also increased with the increase of fine aggregate. In addition, increase in the content of fine aggregate from zero to 15% resulted in the increases of the compressive strength from 1.38 MPa to 2.6 MPa, whilst the increase in the content of coarse aggregate did not apparently

affect the compressive strength. Coarse aggregate is therefore a better ingredient for producing thermal insulation material owing to its lower thermal conductivity and relative higher compressive strength.

(5) It was observed that the moisture content increased when the fiber length increased from 3 mm to 19 mm. Increasing the fiber contents from 0.5% to 2.0% in the FLGC samples resulted in higher moisture absorption. Both of these two variations can be explained by the capillary action which resulted from the polypropylene fibers. Increase in the contents of fine and coarse aggregates from 5% to 15% reduced and increased the moisture absorption respectively, which was resulted from the opposite variations of dry density with the aggregates. The moisture content decreased from 3.5% for sample without waterproofing to 0.94% for specimen with surface waterproofing treatment at 24 h in the chamber with the dry bulb temperature of 35±0.3 ^{o}C and the relative humidity of 90±1.5%. The moisture absorption can be considerably reduced by surface waterproofing treatment, and the difference of moisture contents for FLGC samples with different fiber contents also decreased. Therefore, surface waterproofing treatment can be applied to the thermal insulation material with high water absorption properties which could result in decreased thermal insulating capacity.

Acknowledgements

This study was financially supported by the National Natural Science Foundation of China (51978653, 51204170) and National 111 Project (B14021).

References:

[1] R. Ruparathna, K. Hewage, R. Sadiq, Improving the energy efficiency of the existing building stock: A critical review of commercial and institutional buildings, Renew Sust Energ Rev 53 (2016) 1032-1045.

[2] M.R. Ahmad, B. Chen, S.F.A. Shah, Investigate the influence of expanded clay aggregate and silica fume on the properties of lightweight concrete, Constr Build Mater 220 (2019) 253-266.

[3] Z.H. Zhang, J.L. Provis, A. Reid, H. Wang, Geopolymer foam concrete: An emerging material for sustainable construction, Constr Build Mater 56 (2014) 113-127.

[4] J. Davidovits, Geopolymers: inorganic polymeric new materials, J Therm Anal Calorim 37(8) (1991) 1633-1656.

[5] X.Y. Zhuang, L. Chen, S. Komarneni, C.H. Zhou, D.S. Tong, H.M. Yang, W.H. Yu, H. Wang, Fly ash-based geopolymer: clean production, properties and applications, J Clean Prod 125 (2016) 253-267.

[6] B.C. McLellan, R.P. Williams, J. Lay, A. van Riessen, G.D. Corder, Costs and carbon emissions for geopolymer pastes in comparison to ordinary portland cement, J Clean Prod 19(9-10) (2011) 1080-1090.

[7] R.A. Aguilar, O.B. Diaz, J.I.E. Garcia, Lightweight concretes of activated metakaolin-fly ash binders, with blast furnace slag aggregates, Constr Build Mater 24(7) (2010) 1166-1175.

[8] M.Y.J. Liu, U.J. Alengaram, M.Z. Jumaat, K.H. Mo, Evaluation of thermal conductivity, mechanical and transport properties of lightweight aggregate foamed geopolymer concrete, Energ Buildings 72 (2014) 238-245.

[9] M.Y.J. Liu, U.J. Alengaram, M. Santhanam, M.Z. Jumaat, K.H. Mo, Microstructural investigations of palm oil fuel ash and fly ash based binders in lightweight aggregate foamed geopolymer concrete, Constr Build Mater 120 (2016) 112-122.

[10] Z.H. Zhang, J.L. Provis, A. Reid, H. Wang, Mechanical, thermal insulation, thermal resistance and acoustic absorption properties of geopolymer foam concrete, Cement Concrete Comp 62 (2015) 97-105.

[11] P. Posi, C. Ridtirud, C. Ekvong, D. Chammanee, K. Janthowong, P. Chindaprasirt, Properties of lightweight high calcium fly ash geopolymer concretes containing recycled packaging foam, Constr Build Mater 94 (2015) 408-413.

[12] D.M.A. Huiskes, A. Keulen, Q.L. Yu, H.J.H. Brouwers, Design and performance evaluation of ultra-lightweight geopolymer concrete, Mater Design 89 (2016) 516-526.

[13] B. Nematollahi, R. Ranade, J. Sanjayan, S. Ramakrishnan, Thermal and mechanical properties of sustainable lightweight strain hardening geopolymer composites, Arch Civ Mech Eng 17(1) (2017) 55-64.

[14] N.N. Shao, Y.B. Zhang, Z. Liu, D.M. Wang, Z.T. Zhang, Fabrication of hollow microspheres filled fly ash based foam geopolymers with ultra-low thermal conductivity and relative high strength, Constr Build Mater 185 (2018) 567-573.

[15] R.T.T. Fongang, J. Pemndje, P.N. Lemougna, U.C. Melo, C.P. Nanseu, B. Nait-Ali, E. Kamseu, C. Leonelli, Cleaner production of the lightweight insulating composites: Microstructure, pore network and thermal conductivity, Energ Buildings 107 (2015) 113-122.

[16] Y.J. Huang, L.L. Gong, L. Shi, W. Cao, Y.L. Pan, X.D. Cheng, Experimental investigation on the influencing factors of preparing porous fly ash-based geopolymer for insulation material, Energ Buildings 168 (2018) 9-18.

[17] R.H. Kupaei, U.J. Alengaram, M.Z. Bin Jumaat, H. Nikraz, Mix design for fly ash based oil palm shell geopolymer lightweight concrete, Constr Build Mater 43 (2013) 490-496.

[18] A. Hajimohammadi, T. Ngo, A. Kashani, Sustainable one-part geopolymer foams with glass fines versus sand as aggregates, Constr Build Mater 171 (2018) 223-231.

[19] F. Colangelo, G. Roviello, L. Ricciotti, V. Ferrandiz-Mas, F. Messina, C. Ferone, O. Tarallo, R. Cioffi, C.R. Cheeseman, Mechanical and thermal properties of lightweight geopolymer composites,

Cement Concrete Comp 86 (2018) 266-272.

[20] A. Wongsa, Y. Zaetang, V. Sata, P. Chindaprasirt, Properties of lightweight fly ash geopolymer concrete containing bottom ash as aggregates, Constr Build Mater 111 (2016) 637-643.

[21] A. Wongsa, V. Sata, B. Nematollahi, J. Sanjayan, P. Chindaprasirt, Mechanical and thermal properties of lightweight geopolymer mortar incorporating crumb rubber, J Clean Prod 195 (2018) 1069-1080.

[22] A. Wongsa, V. Sata, P. Nuakiong, P. Chindaprasirt, Use of crushed clay brick and pumice aggregates in lightweight geopolymer concrete, Constr Build Mater 188 (2018) 1025-1034.

[23] J.G. Sanjayan, A. Nazari, L. Chen, G.H. Nguyen, Physical and mechanical properties of lightweight aerated geopolymer, Constr Build Mater 79 (2015) 236-244.

[24] M.M.A. Abdullah, K. Hussin, M. Bnhussain, K.N. Ismail, Z. Yahya, R.A. Razak, Fly Ash-based Geopolymer Lightweight Concrete Using Foaming Agent, Int J Mol Sci 13(6) (2012) 7186-7198.

[25] M.M.A. Abdullah, M.F.M. Tahir, K. Hussin, M. Binhussain, I.G. Sandu, Z. Yahya, A.V. Sandu, Fly Ash Based Lightweight Geopolymer Concrete Using Foaming Agent Technology, Rev Chim-Bucharest 66(7) (2015) 1001-1003.

[26] A. Fernandez-Jimenez, A. Palomo, M. Criado, Microstructure development of alkali-activated fly ash cement: a descriptive model, Cement Concrete Res 35(6) (2005) 1204-1209.

[27] S.E. Gustafsson, Transient plane source techniques for thermal conductivity and thermal diffusivity measurements of solid materials, Review of Scientific Instruments 61(3) (1991) 797-804.

[28] T.J. Sullivan, Introduction to Uncertainty Quantification, Springer, Switzerland, 2015.

[29] T.T. Nguyen, H.H. Bui, T.D. Ngo, G.D. Nguyen, Experimental and numerical investigation of

influence of air-voids on the compressive behaviour of foamed concrete, Mater Design 130 (2017) 103-119.

[30] U. Rattanasak, P. Chindaprasirt, Influence of NaOH solution on the synthesis of fly ash geopolymer, Miner Eng 22(12) (2009) 1073-1078.

[31] K. Somna, C. Jaturapitakkul, P. Kajitvichyanukul, P. Chindaprasirt, NaOH-activated ground fly ash geopolymer cured at ambient temperature, Fuel 90(6) (2011) 2118-2124.

[32] D. Hardjito, S.E. Wallah, D.M.J. Sumajouw, B.V. Rangan, On the development of fly ash-based geopolymer concrete, Aci Mater J 101(6) (2004) 467-472.

[33] J. He, Y.X. Jie, J.H. Zhang, Y.Z. Yu, G.P. Zhang, Synthesis and characterization of red mud and rice husk ash-based geopolymer composites, Cement Concrete Comp 37 (2013) 108-118.

[34] E. Alvarez-Ayuso, X. Querol, F. Plana, A. Alastuey, N. Moreno, M. Izquierdo, O. Font, T. Moreno, S. Diez, E. Vazquez, M. Barra, Environmental, physical and structural characterisation of geopolymer matrixes synthesised from coal (co-)combustion fly ashes, J Hazard Mater 154(1-3) (2008) 175-183.

[35] M. Hassanpour, P. Shafigh, H. Bin Mahmud, Lightweight aggregate concrete fiber reinforcement - A review, Constr Build Mater 37 (2012) 452-461.

[36] H.K. Lee, S.Y. Song, Performance Characteristics of Lightweight Aggregate Cellular Concrete Containing Polypropylene Fibers, J Reinf Plast Comp 29(6) (2010) 883-898.

[37] M.K. Yew, H. Bin Mahmud, P. Shafigh, B.C. Ang, M.C. Yew, Effects of polypropylene twisted bundle fibers on the mechanical properties of high-strength oil palm shell lightweight concrete, Mater Struct 49(4) (2016) 1221-1233.

[38] T. Wu, X. Yang, H. Wei, X. Liu, Mechanical properties and microstructure of lightweight aggregate concrete with and without fibers, Constr Build Mater 199 (2019) 526-539.

[39] G.L. Xue, E. Yilmaz, W. Song, E. Yilmaz, Influence of fiber reinforcement on mechanical behavior and microstructural properties of cemented tailings backfill, Constr Build Mater 213 (2019) 275-285.

[40] M. Aslam, P. Shafigh, M.A. Nomeli, M.Z. Jumaat, Manufacturing of high-strength lightweight aggregate concrete using blended coarse lightweight aggregates, J Build Eng 13 (2017) 53-62.

[41] R. Ahmmad, U.J. Alengaram, M.Z. Jumaat, N.H.R. Sulong, M.O. Yusuf, M.A. Rehman, Feasibility study on the use of high volume palm oil clinker waste in environmental friendly lightweight concrete, Constr Build Mater 135 (2017) 94-103.

[42] M. Medeiros, P. Helene, Efficacy of surface hydrophobic agents in reducing water and chloride ion penetration in concrete, Mater Struct 41(1) (2008) 59-71.